Antipsychotic-induced epigenomic reorganization in frontal cortex samples from individuals with schizophrenia

Bohan Zhu[1,6], Richard I. Ainsworth[2,6], Zengmiao Wang[2], Salvador Sierra[4], Chengyu Deng[1], Luis F. Callado[5], J. Javier Meana[5], Wei Wang[2,3,7], Chang Lu[1,7], Javier González-Maeso[4,7]

[1]Department of Chemical Engineering, Virginia Tech, Blacksburg, VA 24061, USA
[2]Department of Chemistry and Biochemistry, University of California, San Diego, La Jolla, CA 92093, USA
[3]Department of Cellular and Molecular Medicine, University of California, San Diego, La Jolla, CA 92093, USA
[4]Department of Physiology and Biophysics, Virginia Commonwealth University School of Medicine, Richmond, VA 23298, USA
[5]Department of Pharmacology, University of the Basque Country UPV/EHU, CIBERSAM, Biocruces Health Research Institute, E-48940 Leioa, Bizkaia, Spain

[6]These authors contributed equally
[7]These authors jointly supervised this work:
wei-wang@ucsd.edu (W.W.)
changlu@vt.edu (C.L.)
javier.maeso@vcuhealth.org (J.G.-M)

Genome wide association studies have revealed >150 loci associated with schizophrenia risk[1-4], yet these genetic factors do not seem to be sufficient to fully explain the molecular determinants behind this psychiatric condition. Epigenetic marks such as post-translational histone modifications remain largely plastic during development and adulthood, allowing a dynamic impact of environmental factors, including antipsychotic medications, on access to genes and regulatory elements[5,6]. However, no study so far has profiled cell-specific genome-wide histone modifications in postmortem brain samples from schizophrenia subjects or the effect of antipsychotic treatment on such epigenetic marks. Here we show the first comprehensive epigenomic characterization of the frontal cortex of 29 individuals with schizophrenia and 29 matched controls, including histone modifications associated with active promoters and enhancers H3K4me3 and H3K27ac along with RNA expression in neuronal and glial nuclei. Schizophrenia subjects exhibited thousands of cell type-specific epigenetic differences at regions that included several susceptibility genetic loci, such as *NRG1, RGS4* and *HTR2A*. Comparing untreated and treated schizophrenia subjects with controls, our findings provide entirely new insights into differentially modified genes associated with unexpected pathways that are potential markers of antipsychotic treatment. Additionally, we show that the effect of age on the epigenomic landscape is more pronounced in frontal cortex samples of antipsychotic-treated schizophrenia subjects. Together, our data provide important evidence of epigenetic alterations in the frontal cortex of individuals with schizophrenia, and remark the impact of age and antipsychotic treatment on chromatin organization.

Schizophrenia has traditionally been viewed as a genetic disorder, with heritability rates estimated at ~73%[7]. However, previous genome-wide association studies (GWAS) clearly showed a relatively low number of genetic regions associated with schizophrenia risk – these include 108 loci in the first study[1] that have been expanded to over 180 regions[2-4]. Most of these genetic variants were located in non-coding regions and hence, with a few exceptions there is little evidence supporting that coding variants contribute to schizophrenia risk, which also suggests that genetic factors do not seem to be sufficient to fully explain the molecular causes underlying this severe psychiatric condition.

Twin studies have provided evidence that environmental factors contribute to schizophrenia susceptibility. Thus, it had originally been suggested that monozygotic twins, whose DNA

sequences are ~100% identical, have a concordance for schizophrenia of nearly 50%[8,9], yet the most recent work reported a probandwise concordance rate of 33% in monozygotic twins and 7% in dizygotic twins[10]. While such results indicate an important contribution of genetic factors to the etiology of schizophrenia, they argue for a significant role of environmental events in the development of this complex disease. This concept is further supported by epidemiological studies suggesting that prenatal environmental insults, such as maternal infection[11] and severe adverse life events[12], increase the risk of schizophrenia in the offspring.

Gene expression is regulated by the ability of the transcriptional machinery to access DNA, which is tightly packed into chromatin. The status of chromatin organization depends on epigenetic factors, such as DNA methylation and histone modifications that primarily occur on amino-terminal tails[13,14]. Hence these epigenetic mechanisms lead to stable changes in gene expression that are mediated via altered chromatin structure without modification of DNA sequence, and remain largely plastic throughout all periods of brain development and aging. It is then tempting to speculate that epigenetic mechanisms mediate, at least in part, the effects of environmental factors on CNS gene activity, and are therefore potentially involved in the pathophysiology of schizophrenia and other mental illnesses.

Supporting this concept, previous studies reported alterations in chromatin structure and accessibility in tissue samples from schizophrenic subjects and controls. Most of these previous reports, however, were focused on DNA methylation differences in peripheral blood[15] and brain[16]. Using the assay for transposase-accessible chromatin sequencing (ATAC-seq) in bulk tissue homogenates of postmortem frontal cortex samples, only a few differences in chromatin accessibility were observed between schizophrenia subjects and controls, in contrast to thousands of age-related differential accessible chromatin regions[17]. Although interesting, the ATAC-seq approach does not provide the same chromatin state information as histone modifications mapped by chromatin immunoprecipitation sequencing (ChIP-seq) assays do. As an example, it has been suggested that certain histone marks important in cell differentiation are not reflected by ATAC-seq chromatin accessibility data analysis[18].

Recent work combined fluorescence-activated cell sorting (FACS) of neuronal and non-neuronal cell nuclei with histone ChIP-seq assays in two brain regions (prefrontal cortex and anterior cingular cortex) from postmortem brain samples of subjects without any known neurological or psychiatric disease[19]. Besides the identification of cell and region-specific histone modification landscapes in this cohort of control subjects, these findings also compared their datasets with previous GWAS of individuals with psychiatric conditions, reporting that strong specific

enrichments occurred with schizophrenia and weaker associations with depression in both histone H3 acetylation of lysine 27 (H3K27ac) and histone H3 trimethylation of lysine 4 (H3K4me3) peaks. This correlation was almost exclusively observed in neuronal chromatin, but not in non-neuronal cell nuclei. Unfortunately, no study so far has performed epigenomic and transcriptomic profiling in with cell type-specificity of individuals with schizophrenia and controls. Additionally, these previous epigenomic studies in postmortem human brain samples did not address the potential effect of previous exposure to antipsychotics on regulation of chromatin state. This is particularly relevant considering that repeated administration of antipsychotic medications leads to epigenetic modifications at selected gene regions in mouse [20,21] and postmortem human brain[22,23] samples.

Combining MOWChIP-seq[24,25] and Smart-seq2[26] for low-input profiling of histone modifications and transcriptomes, respectively, here we present the first dataset with cell type-specific epigenomic and transcriptomic landscapes in postmortem frontal cortex samples from two cohorts of schizophrenics either previously treated or not with antipsychotic medications and control subjects individually matched by sex and age.

Epigenome and transcriptome profiling in neuronal and glial nuclei from prefrontal cortex of schizophrenia subjects and controls

Prefrontal cortex is a brain region involved in processes affected in schizophrenia patients, such as perception, cognition and sensorimotor gating[27]. We selected bilateral prefrontal cortex (Brodmann area 9) gray matter from 58 brain samples (29 schizophrenia and 29 controls). Control subjects were individually matched based on sex and age, and to a lower degree on postmortem delay (time between death and tissue sample collection) (Supplementary Tables 1 and 2). Nuclei were FACS-sorted using an anti-NeuN antibody as a marker of neuronal nuclei, and NeuN-positive ($NeuN^+$) and NeuN-negative ($NeuN^-$) nuclei (approximately 60,000 nuclei per $NeuN^+$ or $NeuN^-$ sample) were collected for ChIP-seq (10,000 nuclei per library) and RNA-seq (6,000 nuclei per library) (**Fig. 1a**). After library preparation and sequencing, our data demonstrate that the MOWChIP-seq device generates high-quality ChIP-seq data with average unique reads of 13,450,885 and 11,238,429 for the covalent histone modifications H3K27ac and H3K4me3, respectively. These yields were comparable to those in our previous studies using mouse frontal cortex and mammalian tissue culture samples[25,28]. The average Pearson's correlations between replicates were 0.923 and 0.971 for H3K27ac and H3K4me3, respectively, which compare well with those of ENCODE data[29].

Using all prefrontal cortex samples from the 29 control subjects, we analyzed the expression of selected neuron- and glia-specific marker genes. Highly significant (median p-value = 6×10^{-7}) pair-wise differences in molecular marker expression were observed for all markers ranging from mature, functional and synaptic neuron markers to astrocyte, oligodendrocyte and microglial markers (**Fig. 1b** and supplementary Table 3) – confirming neuronal and glial cell-type identities in the $NeuN^+$ and $NeuN^-$ nuclei samples, respectively.

To gain insight into the cell type-specific epigenomic changes associated with schizophrenia, we profiled histone marks H3K27ac and H3K4me3 and transcriptomes in neuronal and glial nuclei of the prefrontal cortex of schizophrenia subjects and controls. Our results revealed a significant number of differential H3K27ac peaks (11,942 in neurons and 3,158 in glia) with the majority of them (11,772 in neurons and 2,969 in glia) having elevated signal in the schizophrenia cohort (**Fig. 1c** and supplementary Table 4). In contrast, there were fewer differences in H3K4me3 (595 in neurons and 73 in glia), yet most (566 in neurons and 73 in glia) also had higher signal in schizophrenia subjects as compared to controls (**Fig. 1c** and supplementary Table 4). We also found a substantial number of differentially expressed genes (DEGs) between schizophrenia subjects and controls, particularly in neuronal nuclei (**Fig. 1c** and supplementary Table 4). The genome browser showed that the schizophrenia group has varied H3K27ac/H3K4me3 levels and RNA-seq reads compared to controls at various loci involved in processes related to synaptic plasticity and cognitive processes or previously associated with schizophrenia risk[30] – these included increased H3K27ac at *NRG1, GRM3*, *RGS4* and *HTR2A* in neuronal nuclei, increased H3K4me3 at *CACNA1C* in neuronal nuclei, and decreased *BDNF* mRNA in glial nuclei (**Figs. 1d,e** and supplementary Table 4).

For integrative analysis of these diverse epigenomic and transcriptomic data, we next employed an unbiased method called *EpiSig*[31], which combines the epigenomic and transcriptomic dataset into a single analysis to cluster regions with similar epigenomic profiles across all the neuronal and glial nuclei samples. 85,462 signal enriched regions were grouped into 814 epigenomic clusters covering 14.53% of the genome. These clusters were further combined into 6 groups (sections) using the K-means method (**Fig. 2a** and supplementary Table 5). Section I had high coverage in intron, intergenic regions and open sea, indicating the inactive regions. It was also enriched in chromosome X compared to other sections. Section III was highly enriched in enhancers, and low coverage in intergeneric regions, which is likely associated with active enhancers given high signal of H3K27ac. Section IV also had high coverage of enhancers (**Fig. 2b** and supplementary Table 5). However, CpG island showed high proportion in this section,

indicating active promoters. As for the average differential signals across sections, a great variance was observed. For example, the signal of H3K4me3 was higher in schizophrenia subjects compared to controls for neuronal nuclei in section V, while it was lower in schizophrenia subjects for glial samples (**Fig. 2b** and supplementary Table 5).

Transcriptional regulatory processes proceed as a hierarchy of orchestrated events that ultimately modulate the expression of downstream target genes. Using the recently developed *Taiji* algorithm[32], which allows access to information pertaining to transcriptional cascades deriving from upstream drivers through specific pathway mechanisms to downstream effects, we integrated epigenomic and transcriptomic data to construct 116 individual transcriptional networks in neuronal and glial nuclei from schizophrenia subjects and controls. We identified active promoters and enhancers using H3K27ac and then predicted transcription factor (TF) binding sites by scanning 1,165 TF motifs linking putative TF binding sites to their targets using *EpiTensor*[33], an unsupervised method to predict enhancer-promoter associations. TFs were subsequently ranked according to regulatory importance using the Personalized PageRank (PPR) algorithm for each unique network topology[34], as well as absolute change in schizophrenia *vs* control PPR score for those driver TFs with significant case/control change in PPR score for matched pairs of neuronal and glial nuclei (**Fig. 2c** and supplementary Table 6 – top 22 TFs for each cell type). Of the top 22 neuronal TFs, 19 were found to be cell-type specific and involved in processes such as "*Deactivation of β-catenin transactivating complex*" (p-value 2.62×10^{-3}), including SOX2 and TCF7L2 (**Fig. 2d** and supplementary Table 6). Cytokine signaling TFs were also enriched including those involved in "*IL-4 and IL-13 signaling*" (p-value 1.31×10^{-6}) (TFs: SOX2, ZEB1 and FOXO1) (**Fig. 2d** and supplementary Table 6). Furthermore, the glial-specific TFs were enriched in differentiation pathways including *"Positive regulation of myeloid cell differentiation*" (p-value 2.24×10^{-6}) (TFs: FOXO3, STAT3, TAL1 and FOS) (**Fig. 2e** and supplementary Table 6) in line with the previously suggested aberrant functioning of myeloid immune cells in schizophrenia patients[35]. Consistent with the known roles of apoptosis in schizophrenia pathogenesis[36], we also obtained the pathway *"Positive regulation of neuron death"* in glial cells (p-value 9.55×10^{-5}) (TFs: FOXO3, ASCL1 and FOS) (**Fig. 2e** and supplementary Table 6).

Schizophrenia-associated epigenetic alterations recovered by antipsychotic treatment

Using preclinical models, it has been suggested that chronic antipsychotic drug administration leads to long lasting changes in frontal gene expression and chromatin organization[20,23], but the epigenomic consequences of antipsychotic treatment in postmortem human brain samples

remain largely unexplored. Collectively, our findings affirm that the neuronal and glial epigenomic and transcriptomic landscapes are affected by antipsychotic treatment (**Extended Data Fig. 1** and supplementary Table 7). To further determine the functional relevance of antipsychotic treatment, we aimed to identify the biological pathways dysregulated in the antipsychotic-free (AF) schizophrenia group that were also reversed to control levels in the antipsychotic-treated (AT) schizophrenia group as compared to individually matched controls. We conducted analysis of the neuronal nuclei from AF-schizophrenia/control pairs to obtain a rank-ordered list of driver TFs based on significance between case and control PPR. In conjunction with this, analysis of those TFs that had no statistically significant variation in neuronal nuclei from the AT-schizophrenia/control pair cohort allowed for further filtering and the identification of 4 top TFs with changes in the AF-schizophrenia/control group but not in the AT-schizophrenia/control group (ZNF32, ZNF525, ZNF416 and ZEB1) (**Figs. 3a,i** and supplementary Table 8). As an example related to the functional relevance of these findings, TF ZNF32, which behaves as an effective autophagy inhibitor[37], showed a lower PPR in untreated schizophrenics compared to controls (p-value = 8.1×10^{-3}) (**Figs. 3a,i** and supplementary Table 8). This regulatory influence was restored by antipsychotic treatment as shown with no significant difference between case and control in the AT-schizophrenia group (p-value = 5.8×10^{-1}) (**Fig. 3i** and supplementary Table 8).

We also identified a total of 17 DEG regulatees that were downstream of either the AF-schizophrenia-specific TFs ZNF525 and ZEB1 or the control-specific TFs ZNF32 and ZNF416 (**Figs. 3b** and supplementary Table 8). In parallel, AF-schizophrenia/control DEGs were integrated with genes from the AT-schizophrenia/control cohort with no case/control differences in expression resulting in a list of 116 cohort-specific DEGs (**Fig. 3b** and supplementary Table 8). Functional enrichment analysis of the union of 131 genes resulted in pathways involved in glutamatergic neurotransmission including *"Activation of AMPK downstream of NMDARs"* (p-value 2.94×10^{-5}) (**Fig. 3j** and supplementary Table 8). Structural and functional modifications of dendritic spines are central to brain development and plasticity[38]. Studies from postmortem brains of subjects with neurodevelopmental disorders including schizophrenia demonstrate altered density and morphology of dendritic spines, particularly in the frontal cortex[39,40]. IQGAP scaffold proteins facilitate the formation of complexes that regulate cytoskeletal dynamics including microtubules[41]. Interestingly, the most significant pathway restored in the AT-schizophrenia group was "*Rho GTPases activate IQGAPs*" (p-value = 2.26×10^{-6}) (**Fig. 3j** and supplementary Table 8). The importance of this pathway was validated by the analysis of the

clusters from the *EpiSig* pipeline. Thus, taking the top 3 clusters ranked for enrichment in each histone mark and mapping their differential peaks to genes resulted in 294 genes enriched in pathways including *"Adherens junctions interactions"* (p-value 1.22×10^{-4}) (**Extended Data Fig. 2** and supplementary Table 9).

Autophagy has been suggested to play an important role in the pathophysiology of schizophrenia and antipsychotics are known to modulate the process[42]. Notably, the pathways *"Aggrephagy"* (p-value 1.34×10^{-4}) and *"Macroautophagy"* (p-value 1.70×10^{-4}) were significantly enriched (**Fig. 3j** and supplementary Table 8). Expression of the *"Macroautophagy"* genes *ATG16L2*, *AMBRA1*, *PRKAB1*, *TUBA1A*, *TUBB2A,* and *TUBA4A* was restored in the AT-schizophrenia group (**Fig. 3n** and supplementary Table 8). Ubiquitin B (UBB) expression has been previously identified as a strong correlate of schizophrenia symptoms[43]. We show a 1.96-fold decrease specific to AF-schizophrenics compared to controls (p-value = 4.0×10^{-2}) and regulation by the upstream TFs ZNF525 and ZNF416 (Supplementary Table 8).

Glial cells modulate and act as effectors in neurodevelopment through a wide range of neuronal-glial cell interactions. Using the same process as above, we identified 2 driver TFs with significant change in PPR between case and control for the AF-schizophrenia cohort and no significant difference between case and control in the AT-schizophrenia group (SOX11 and NR1H3; **Fig. 3c,i** and supplementary Table 8). 75 downstream DEG regulatees of these two TFs were identified in the AF cohort showing significant regulatory case/control change. In parallel 102 cohort-specific DEGs were identified as AF-schizophrenia/control DEG and having no significant difference in expression in the AT-schizophrenia/control cohort (**Fig. 3d** and supplementary Table 8). Functional enrichment analysis of the union of 153 genes included "*Post NMDA receptor activation events*" (p-value = 6.91×10^{-4}), and "*Kinesins*" (p-value = 6.76×10^{-3}) whose typical function is to transport cargo along microtubules[44] (**Fig. 3k** and supplementary Table 8). These findings, together with the alterations in tubulin genes observed neuronal nuclei of AF-schizophrenia subjects (**Fig. 3n** and supplementary Table 8), suggest the existence of epigenetic alterations in the context of cortical dendritic structural plasticity that are reversed by antipsychotic treatment.

Epigenetic alterations that represent a consequence of antipsychotic treatment

We next sorted to characterize those TFs that exhibit regulatory alterations in the AT-schizophrenia/control cohort but not in the AF-schizophrenia/control cohort. Our goal was to identify modifications in pathways that represent a consequence of antipsychotic medication rather that an epigenetic mark of schizophrenia in postmortem human brain. In the same way as

above, we rank-ordered driver TFs based on significance between case and control PPR for the neuronal nuclei from AT-schizophrenia/control pairs. Again, those TFs that showed no disease significance in the AF-schizophrenia cohort were selected yielding the 2 top ranked TFs *FOXO1* (PPR AT-schizophrenia > controls) (p-value = 1.45×10^{-3}) and *Calcium-Response Factor* (*CARF*) (PPR AT-schizophrenia < controls) (p-value = 2.06×10^{-2}) (**Figs. 3e,i** and supplementary Table 8).

We identified dysregulated AT-schizophrenia/control DEG regulatees of these TFs in neuronal nuclei via analysis of differential edge weights thus obtaining 81 genes (**Fig. 3f** and supplementary Table 8). AT-treated/control DEGs were intersected with genes from the AF-schizophrenia/control cohort with no case/control differences in expression resulting in a list of 41 cohort-specific DEGs (**Fig. 3f** and supplementary Table 8). Pathway analysis on the union of genes yields the pathway *"Regulation of p53 activity"* (p-value 3.93×10^{-3}) (**Figs. 3l** and supplementary Table 8), including the FOXO1 AT-schizophrenia/control cohort DEG regulatees *CCNA1, BLM, TP53RK*, *RBBP8* and *PDK1* (**Fig. 3o** and supplementary Table 8), and the AT-schizophrenia/control cohort-specific DEGs *PRKAA1* and *TAF15* (Supplementary Table 8). p53 is one of the most critical pro-apoptotic genes, and antipsychotics are known to produce complex effects including the activation of both proapoptotic and antiapoptotic signaling pathways[45]. Our data showed that all genes involved in the regulation of p53 presented a significantly lower expression in AT-schizophrenics compared to controls (Supplementary Table 8), suggestive of a repressive role for FOXO1 for its 5 regulatees, as FOXO1 had higher PPR in treated schizophrenics (**Figs. 3e,l** and supplementary Table 8) and was also 2.38-fold more highly expressed in schizophrenics for the treated-cohort (p-value = 1.07×10^{-2}) (Supplementary Table 8). Analysis of the clusters from the *EpiSig* pipeline for the AT-schizophrenia/control cohort corroborated alterations in pathways related to p53[46] (**Extended Data Fig. 3** and supplementary Table 10).

In glial cells, selection of TFs that showed significant difference in the AT-schizophrenia/control cohort but not in the AF-schizophrenia/control cohort yielded 3 driver TFs (PRDM4, NFYC and ZNF510) differentially regulating 119 downstream AT-schizophrenia/control DEG regulatees (**Figs. 3g,i** and supplementary Table 8). Furthermore, 116 genes cohort-specific DEGs identified as AT-schizophrenia/control DEGs and having no significant difference in expression in the AF-schizophrenia/control cohort (**Figs. 3g,i** and supplementary Table 8). Enriched pathways derived from this union of genes included *"PERK regulates gene expression"* (p-value 7.34×10^{-4}) and "*ATF4 activates genes in response to endoplasmic reticulum stress*" (p-value

2.34×10^{-3}) (**Fig. 3m** and supplementary Table 8) – two pathways involved in mechanisms related to neurodegeneration in response to stress[47].

Age differentially affects antipsychotic-treated schizophrenia subjects

In order to assess the effect of age on gene expression, we first compared transcriptomes of subjects with schizophrenia and the controls to evaluate how these changes correlated with age. Within neurons in the control group, we identified 742 genes that were significantly correlated with age – with most of them (573, or 77.2%) showing decreased expression in older control subjects (**Fig. 4a** and supplementary Table 11). The opposite, however, was observed in neurons from schizophrenia subjects with 18 out of 622 (2.8%) in AF-schizophrenia presenting a negative correlation with age, an effect that was partly reversed in the AT-schizophrenia cohort (85 out of 242 or 35.1%) (**Fig. 4a** and supplementary Table 11).

Our data also demonstrate that within the glial genes correlated with age (1031, 389 and 351 in controls, AF-schizophrenia and AT-schizophrenia, respectively), approximately half (491 or 47.6%) were positively correlated with age in the control group whereas a much higher fraction of genes showed increased expression with age in the schizophrenia group, particularly in the AF-schizophrenia cohort (382 or 98.2% in AF-schizophrenia, and 276 or 78.6% in AT-schizophrenia) (**Fig. 4b** and supplementary Table 11). These results suggest that age differentially affects gene expression in the prefrontal cortex of AF-schizophrenia vs AT-schizophrenia subjects as compared to age-matched controls. Importantly, this was further confirmed by functional integration of epigenomic and transcriptomic data and the evaluation of how these alterations correlated with age.

Thus, we evaluated pairwise changes in expression between schizophrenia subjects and their age-matched controls, and identified 206 and 310 genes with an absolute Pearson's correlation of ≥ 0.50 in neuronal nuclei from the AF-schizophrenia/control and AT-schizophrenia/control cohorts, respectively (**Figs. 4c,d** and supplementary Table 11). We also found enriched biological processes associated with age, including "*Regulation of protein kinase activity*" (p-value 6.69×10^{-7}) in the AT-schizophrenia/control group (**Fig. 4e** and supplementary Table 11). Within this gene set, the difference between AT-schizophrenia subjects and control pairs correlated either positively (WNK1) or negatively (SFRP2) with age (**Figs. 4f,g** and supplementary Table 11). Evaluation of pairwise changes in PPR identified 48 TFs with high correlations to age in neuronal nuclei from AT-schizophrenia/control cohorts, whereas this alteration was not observed in the AF-schizophrenia/control group (**Figs. 4c,d** and supplementary Table 11). Pathway analysis of the neuronal TFs affected by age in the AT-

schizophrenia/control cohort led to the top pathway "*NGF-simulated transcription*" (p-value 8.04 $\times 10^{-8}$), including the TFs EGR2 and ATF2 (Supplementary Table 11). Hallucinations and delusions typically attenuate with aging[48], which is consistent with the lower PPR difference for EGR2 – a preclinical marker of psychosis-like behavior[49] – that we observed in older subjects (**Fig. 4h** and supplementary Table 11).

In glial nuclei, 147 and 88 genes were identified with AF-schizophrenia/control and AT-schizophrenia/control expression difference vs age correlations of ≥ 0.60, respectively (**Figs. 4i,j** and supplementary Table 11). Enriched pathways in the AT-schizophrenia/control group included: *"Degradation of DVL"* (p-value 4.04 $\times 10^{-5}$) and *"Beta-catenin independent WNT signaling"* (p-value 5.06 $\times 10^{-4}$) (**Fig. 4k** and supplementary Table 11). Since dysfunctional WNT signaling is associated with several CNS disorders including Alzheimer's[50], together, these data also suggest that this positive correlation between glial gene differences in AT-schizophrenia subjects/control pairs and age (**Fig. 4k** and supplementary Table 11) may be responsible for some of the negative effects of antipsychotic treatment on cognitive processes. We also identified 11 and 53 TFs correlated with age in the AF-schizophrenia/control and AT-schizophrenia/control cohorts, respectively (**Figs. 4i,j** and supplementary Table 11). However, as in neuronal nuclei, the effect of age became more evident in the AT-schizophrenia/control group with age-related adaptations in glial TF-affected pathways that included "*Signaling by NOTCH*" (p-value 3.2 $\times 10^{-4}$) (Supplementary Table 11).

Discussion

Understanding the molecular determinants involved in schizophrenia is critical for devising new treatment strategies and the discovery of the pathogenic mechanisms underlying this psychiatric condition. In this study, we combined low-input epigenomic and transcriptomic analysis to define how gene expression and TF regulation vary in schizophrenia subjects relative to controls and in response to antipsychotic treatment and aging. Our data provide, for the first time, evidence suggesting alterations in covalent histone modifications at different gene regions previously associated with schizophrenia risk, as well as additional genes involved in pathways related to immunological and neurodevelopmental processes. Whereas previous studies with postmortem human brain samples compared using indirect methods differences in chromatin accessibility between schizophrenia subjects and controls[17], here we provide epigenomic signatures that distinguish between those observed in AF-schizophrenia subjects as well as alterations that denote previous treatment with antipsychotic medications.

A powerful feature of the *Taiji* framework is to allow analysis of individual samples[32]. We conducted pairwise comparison between schizophrenia and matched controls, which is crucial to tease out treatment- or age-associated effects. This integrative analysis of transcriptomic and epigenomic data at the systems level uncovered key regulators and important pathways based on their global importance in the genetic networks. We found that transcriptional mechanisms via novel pathways that had not been previously associated with schizophrenia show alterations in AF-schizophrenia subjects, and that these schizophrenia-linked pathways were statistically unaffected in the AT-schizophrenia group, consistent with a potential role of these epigenomic signatures in the clinical efficacy of antipsychotics. Based on our ability to individually match schizophrenia and control pairs by age, we also revealed the intriguing observation that the effect of age on TF regulation of gene expression was significantly more pronounced in AT-schizophrenia subjects as compared to AF-schizophrenia subjects and controls. Additionally, our data highlight processes related to key pathways that may represent a consequence of antipsychotic medication, rather than a reversal of the molecular alterations observed in AF-schizophrenia subjects. These pathways suggest the existence compensatory perturbations that emerge in response to repeated antipsychotic drug administration and ultimately restrain their therapeutic effects[22,23].

In the largest ChIP-seq/RNA-seq study in postmortem brain samples from schizophrenia subjects and controls, we show cell-type specific epigenomic differences in individuals with schizophrenia as well as cellular alterations in signaling pathways potentially involved in either the elimination of schizophrenia-related epigenomic alterations upon antipsychotic drug treatment or the antipsychotic-dependent modulation of alternative epigenetic pathways previously unaffected in the untreated schizophrenia cohort. Building on our data, future research could test the causal role of specific molecular pathways implicated in schizophrenia pathophysiology, as well as the therapeutic versus compensatory or negative side epigenomic outcomes induced by chronic treatment with antipsychotic medications.

Data availability The raw ChIP-seq and RNA-seq data were deposited in dbGaP under accession number phs002487.v1.p1. The processed data can be accessed via Gene Expression Omnibus (GEO) under accession number GSE174407.

Acknowledgements National Institutes of Health R01MH084894 (J.G.-M.), R01MH111940 (J.G.-M.), R01GM143940 (C.L.), R01HG009626 (W.W.), R01AI50282 (W.W.), Basque Government IT1211-19 (J.J.M.), and VCU Presidential Request Fund (J.G.-M.) helped fund this study. The authors thank the staff members of the Basque Institute of Legal Medicine for their cooperation in the study.

Author contributions B.Z., C.L., and J.G.-M. conceived and designed the experiments. R.A., B.Z., Z.W., W.W., C.L., and J.G.-M. analyzed the data and wrote the manuscript. W.W., C.L., and J.G.-M. supervised the research and obtained funding. B.Z., supervised by C.L., performed epigenomic and transcriptomic assays. R.A., supervised by W.W., conducted data analysis and interpreted findings. Z.W., supervised by W.W., and B.Z., supervised by C.L., helped with data analysis. C.D., supervised by C.L., helped with epigenomic and transcriptomic assays. S.S., supervised by C.L. and J.G.-M., helped with nuclear sorting. L.F.C. and J.J.M. obtained and classified postmortem human brain samples. All authors reviewed and approved the final manuscript.

Competing interests J.G.-M. has a sponsored research contract with *NeuRistic*. The remaining authors declare that they have no competing interests.

References

1 Ripke, S. *et al*. Biological insights from 108 schizophrenia-associated genetic loci. *Nature* **511,** 421-427 (2014).

2 Sekar, A. *et al.* Schizophrenia risk from complex variation of complement component 4. *Nature* **530,** 177-183 (2016).

3 Purcell, S. M. *et al.* A polygenic burden of rare disruptive mutations in schizophrenia. *Nature* **506,** 185-190 (2014).

4 Fromer, M. *et al.* De novo mutations in schizophrenia implicate synaptic networks. *Nature* **506,** 179-184 (2014).

5 Tsankova, N. *et al.* Epigenetic regulation in psychiatric disorders. *Nat Rev Neurosci* **8,** 355-367 (2007).

6 Ibi, D. & Gonzalez-Maeso, J. Epigenetic signaling in schizophrenia. *Cell Signal* **27,** 2131-2136 (2015).

7 Sawa, A. & Snyder, S. H. Schizophrenia: diverse approaches to a complex disease. *Science* **296,** 692-695 (2002).

8 Cardno, A. G. & Gottesman, II Twin studies of schizophrenia: from bow-and-arrow concordances to star wars Mx and functional genomics. *Am J Med Genet* **97,** 12-17 (2000).

9 Hallmayer, J. *et al.* Genetic heritability and shared environmental factors among twin pairs with autism. *Arch Gen Psychiatry* **68,** 1095-1102 (2011).

10 Hilker, R. *et al.* Heritability of Schizophrenia and Schizophrenia Spectrum Based on the Nationwide Danish Twin Register. *Biol Psychiatry* **83,** 492-498 (2018).

11 Yudofsky, S. C. Contracting schizophrenia: lessons from the influenza epidemic of 1918-1919. *JAMA* **301,** 324-326 (2009).

12 Malaspina, D. *et al.* Acute maternal stress in pregnancy and schizophrenia in offspring: a cohort prospective study. *BMC Psychiatry* **8,** 71 (2008).

13 Bastle, R. M. & Maze, I. Chromatin Regulation in Complex Brain Disorders. *Curr Opin Behav Sci* **25,** 57-65 (2019).

14 Graff, J. & Tsai, L. H. Histone acetylation: molecular mnemonics on the chromatin. *Nat Rev Neurosci* **14,** 97-111 (2013).

15 Aberg, K. A. *et al.* Methylome-wide association study of schizophrenia: identifying blood biomarker signatures of environmental insults. *JAMA Psychiatry* **71,** 255-264 (2014).

16 Jaffe, A. E. *et al.* Mapping DNA methylation across development, genotype and schizophrenia in the human frontal cortex. *Nat Neurosci* **19,** 40-47 (2016).

17 Bryois, J. *et al.* Evaluation of chromatin accessibility in prefrontal cortex of individuals with schizophrenia. *Nat Commun* **9,** 3121 (2018).

18 Saunders, A. *et al.* Molecular Diversity and Specializations among the Cells of the Adult Mouse Brain. *Cell* **174,** 1015-1030 e1016 (2018).

19 Girdhar, K. *et al.* Cell-specific histone modification maps in the human frontal lobe link schizophrenia risk to the neuronal epigenome. *Nat Neurosci* **21,** 1126-1136 (2018).

20 de la Fuente Revenga, M. *et al.* Chronic clozapine treatment restrains via HDAC2 the performance of mGlu2 receptor agonism in a rodent model of antipsychotic activity. *Neuropsychopharmacology* **44,** 443-454 (2018).

21 Ma, S. *et al.* Cell-type-specific brain methylomes profiled via ultralow-input microfluidics. *Nat Biomed Eng* **2,** 183-194 (2018).

22 Ibi, D. *et al.* Antipsychotic-induced Hdac2 transcription via NF-kappaB leads to synaptic and cognitive side effects. *Nat Neurosci* **20,** 1247-1259 (2017).

23 Kurita, M. *et al.* HDAC2 regulates atypical antipsychotic responses through the modulation of mGlu2 promoter activity. *Nat Neurosci* **15,** 1245-1254 (2012).

24 Cao, Z. *et al.* A microfluidic device for epigenomic profiling using 100 cells. *Nat Methods* **12,** 959-962 (2015).

25 Zhu, B. *et al.* MOWChIP-seq for low-input and multiplexed profiling of genome-wide histone modifications. *Nat Protoc* **14,** 3366–3394 (2019).

26 Picelli, S. *et al.* Smart-seq2 for sensitive full-length transcriptome profiling in single cells. *Nat Methods* **10,** 1096-1098 (2013).

27 Andreasen, N. C. *et al.* Regional brain abnormalities in schizophrenia measured with magnetic resonance imaging. *JAMA* **272,** 1763-1769 (1994).

28 Ma, S. *et al.* Low-input and multiplexed microfluidic assay reveals epigenomic variation across cerebellum and prefrontal cortex. *Sci Adv* **4,** eaar8187 (2018).

29 Consortium. An integrated encyclopedia of DNA elements in the human genome. *Nature* **489,** 57-74 (2012).

30 Farrell, M. S. *et al.* Evaluating historical candidate genes for schizophrenia. *Mol Psychiatry* **20,** 555-562 (2015).

31 Ai, R. *et al.* Comprehensive epigenetic landscape of rheumatoid arthritis fibroblast-like synoviocytes. *Nat Commun* **9,** 1921 (2018).

32 Zhang, K. *et al.* Taiji: System-level identification of key transcription factors reveals transcriptional waves in mouse embryonic development. *Sci Adv* **5,** eaav3262 (2019).

33 Zhu, Y. *et al.* Constructing 3D interaction maps from 1D epigenomes. *Nat Commun* **7,** 10812 (2016).

34 Yu, B. *et al.* Epigenetic landscapes reveal transcription factors that regulate CD8(+) T cell differentiation. *Nat Immunol* **18,** 573-582 (2017).

35 Comer, A. L. *et al.* The Inflamed Brain in Schizophrenia: The Convergence of Genetic and Environmental Risk Factors That Lead to Uncontrolled Neuroinflammation. *Front Cell Neurosci* **14,** 274 (2020).

36 Jarskog, L. F. *et al.* Apoptotic mechanisms in the pathophysiology of schizophrenia. *Prog Neuropsychopharmacol Biol Psychiatry* **29,** 846-858 (2005).

37 Li, Y. *et al.* ZNF32 inhibits autophagy through the mTOR pathway and protects MCF-7 cells from stimulus-induced cell death. *Sci Rep* **5,** 9288 (2015).

38 Spruston, N. Pyramidal neurons: dendritic structure and synaptic integration. *Nat Rev Neurosci* **9,** 206-221 (2008).

39 Black, J. E. *et al.* Pathology of layer V pyramidal neurons in the prefrontal cortex of patients with schizophrenia. *Am J Psychiatry* **161,** 742-744 (2004).

40 Glantz, L. A. & Lewis, D. A. Decreased dendritic spine density on prefrontal cortical pyramidal neurons in schizophrenia. *Arch Gen Psychiatry* **57,** 65-73 (2000).

41 Cao, D. *et al.* Signaling Scaffold Protein IQGAP1 Interacts with Microtubule Plus-end Tracking Protein SKAP and Links Dynamic Microtubule Plus-end to Steer Cell Migration. *J Biol Chem* **290,** 23766-23780 (2015).

42 Merenlender-Wagner, A. *et al.* Autophagy has a key role in the pathophysiology of schizophrenia. *Mol Psychiatry* **20,** 126-132 (2015).

43 Rubio, M. D. *et al.* Dysfunction of the ubiquitin proteasome and ubiquitin-like systems in schizophrenia. *Neuropsychopharmacology* **38,** 1910-1920 (2013).

44 Gigant, B. *et al.* Structure of a kinesin-tubulin complex and implications for kinesin motility. *Nat Struct Mol Biol* **20,** 1001-1007 (2013).

45 Aylon, Y. & Oren, M. Living with p53, dying of p53. *Cell* **130,** 597-600 (2007).

46 Endo, Y. *et al.* Regulation of clathrin-mediated endocytosis by p53. *Genes Cells* **13,** 375-386 (2008).

47 Celardo, I. *et al.* Mitofusin-mediated ER stress triggers neurodegeneration in pink1/parkin models of Parkinson's disease. *Cell Death Dis* **7,** e2271 (2016).

48 Davidson, M. *et al.* Severity of symptoms in chronically institutionalized geriatric schizophrenic patients. *Am J Psychiatry* **152,** 197-207 (1995).

49 Gonzalez-Maeso, J. *et al.* Hallucinogens Recruit Specific Cortical 5-HT(2A) Receptor-Mediated Signaling Pathways to Affect Behavior. *Neuron* **53,** 439-452 (2007).

50 Wan, W. *et al.* The role of Wnt signaling in the development of Alzheimer's disease: a potential therapeutic target? *Biomed Res Int* **2014,** 301575 (2014).

Figure legends

Fig. 1 | Comparison of epigenomic and transcriptomic landscapes in the frontal cortex of schizophrenia subjects and controls. a, Overview of the experimental design starting from postmortem human prefrontal cortex samples to generate cell type-specific H3K27ac, H3K4me3 and RNA profiles. **b,** Heatmap of the expression of neuronal and glial cell markers across all $NeuN^+$ and $NeuN^-$ prefrontal cortex samples from 29 control subjects. **c,** Differential histone modification peaks and DEGs obtained by comparing schizophrenia (n = 29) and controls (n = 29). The differential peaks or differentially expressed genes were identified using FDR < 0.05. **d,** Exemplar genomic track view of H3K27ac, H3K4me3 and RNA signals for matched AF-schizophrenia/control and AT-schizophrenia/control pairs in $NeuN^+$ and $NeuN^-$ cells. 50Mb region displayed: chr1:68,000,000-118,000,000 (GRCh38). **e,** Volcano plots showing genes associated with differential H3K27ac and H3K4me3 peaks and DEGs. The differential peaks were annotated to their nearest genes. Candidate genes for schizophrenia or genes involved in significant GO terms are labeled. The horizontal lines indicate FDR of 0.05.

Fig. 2 | Genome-wide multidimensional clusters in the frontal cortex of schizophrenia subjects and controls. a, Integration analysis using *EpiSig*. *814* EpiSig clusters across 348 genome-wide sequencing datasets were grouped into 6 sections. The heatmap shows the signal in each *EpiSig* cluster (row: *EpiSig* cluster; column: marker) **b,** For each *EpiSig* cluster, from left to right, the heatmaps are: the region percentage in each chromosome; the genomic annotation; the CpG annotation; the percentage of enhancer; the difference signal between schizophrenia and controls in neuronal and glial nuclei. **c,** Bubble plot of normalized PPR (color) and log expression (bubble size) for top 22 significant (p-value < 0.05) neuronal schizophrenia vs control TFs and top 22 significant (p-value < 0.05) glial schizophrenia vs control TFs (41 unique TFs) ranked across 29 schizophrenia and 29 control neuronal and glial nuclei samples. **d,** Overrepresented pathway analysis for 19 neuron-specific TFs. **e,** Overrepresented pathway analysis for 19 glia-specific TFs.

Fig. 3 | Epigenomic alterations affected by antipsychotic treatment. a, Pairwise neuronal differences (schizophrenia – control) in PPR score for top 4 TFs affected in 15 AF-schizophrenia/control pairs, but not in 14 AT-schizophrenia/control pairs. **b,** Number of DEG regulatees by TFs (ZNF32, ZNF416, ZNF525, ZEB1), and number of DEGs in neuronal nuclei from AF-schizophrenia/control pairs. **c,** Pairwise glial differences (schizophrenia – control) in

PPR score for top 2 TFs affected in 15 AF-schizophrenia/control pairs, but not in 14 AT-schizophrenia/control pairs. **d,** Number of DEG regulatees by TFs (SOX11, NR1H3), and number of DEGs in glial nuclei from AF-schizophrenia/control pairs. **e,** Pairwise neuronal differences (schizophrenia – control) in PPR score for top 2 TFs affected in 14 AT-schizophrenia/control pairs, but not in 15 AT-schizophrenia/control pairs. **f,** Number of DEG regulatees by TFs (FOXO1 and CARF), and number of DEGs in neuronal nuclei from AT-schizophrenia/control pairs. **g,** Pairwise glial differences (schizophrenia – control) in PPR score for top 3 TFs affected in 14 AT-schizophrenia/control pairs, but not in 15 AF-schizophrenia/control pairs. **h,** Number of DEG regulatees by TFs (PRDM4, NFYC, ZNF510), and number of DEGs in glial nuclei from AT-schizophrenia/control pairs. **i,** Heatmaps for average pairwise difference (schizophrenia – control) in TF PPR in AF-schizophrenia, AT-schizophrenia and controls in neuronal and glial nuclei with corresponding cohort significance. **j,** Functional enrichment analysis of union of genes from AF-schizophrenia/control pairs in neuronal nuclei. **k,** Functional enrichment analysis of union of genes from AF-schizophrenia/control pairs in glial nuclei. **l,** Functional enrichment analysis of union of genes from AT-schizophrenia/control pairs in neuronal nuclei. **m,** Functional enrichment analysis of union of genes from AT-schizophrenia/control pairs in glial nuclei. **n,** Pairwise expression difference (schizophrenia – control) of an exemplar AF-schizophrenia/control cohort DEG (TUBB2A) across all 29 schizophrenia-control pairs in neuronal nuclei. **o,** H3K27ac tracks for PDK1 (member of the 81 gene set in **f**) in neuronal nuclei. Box highlighting the FOXO1 DNA-binding motif in promoter at position chr2: 172,555,706 – 172,555,718 (GRCh38). Two exemplar AT-schizophrenia/control cohort pairs showing differential ATAC peak intensity around motif locus and an example AF-schizophrenia/control cohort patient pair with no difference.

Fig. 4 | Epigenomic effect of age on treated schizophrenia subjects. a, Violin plots for Pearson's R correlation coefficients of age *vs* expression for 742, 622 and 242 genes from control, AF-schizophrenia, and AT-schizophrenia neuronal nuclei, respectively. **b,** Violin plots for Pearson's R correlation coefficients of age *vs* expression for 1031, 389 and 351 genes from control, AF-schizophrenia, and AT-schizophrenia glial nuclei, respectively **c,** Number of pairwise TF PPR and pairwise gene expression differences correlated with age in neuronal nuclei from AF-schizophrenia/control pairs. **d,** Number of pairwise TF PPR and pairwise gene expression differences correlated with age in neuronal nuclei from AT-schizophrenia/control pairs. **e,** Heatmap for the 14 age positively-correlated (schizophrenia - control increase with age) and 12 age negatively-correlated (schizophrenia - control decrease with age) genes of the significant

GO term "*Regulation of kinase activity*" from the AT-schizophrenia/control neuronal cohort. **f,** Example gene, WNK1 pairwise expression difference (schizophrenia - control) vs age (Pearson's R = 0.73; p-value = 0.003). **g,** Example gene, SFRP2 pairwise expression difference (schizophrenia - control) vs age (Pearson's R = -0.70; p-value = 0.005). **h,** Example TF, EGR2 pairwise PPR difference (schizophrenia - control) vs age (Pearson's R = 0.69; p-value = 0.0003 **i,** Number of pairwise TF PPR and pairwise gene expression differences correlated with age in glial nuclei from AF-schizophrenia/control pairs. **i,** Number of pairwise TF PPR and pairwise gene expression differences correlated with age in glial nuclei from AT-schizophrenia/control pairs. **k,** Heatmap for the 5 age positively-correlated (schizophrenia - control increase with age) genes of the significant GO term "*Beta-catenin independent WNT signaling*" from the AT-schizophrenia/control glial cohort.

Supplementary Material

Methods

Data reporting

No statistical methods were used to predetermine sample size. The experiments including schizophrenia and control pairs were not randomized, and the investigators were not blinded to allocation during experiments and outcome assessment.

Post-mortem Human Brain Tissue Samples

Human brains were obtained during autopsies performed at the Basque Institute of Legal Medicine, Bilbao, Spain. The study was developed in compliance with policies of research and ethical review boards for post-mortem brain studies (Basque Institute of Legal Medicine, Spain). Deaths were subjected to retrospective searching for previous medical diagnosis and treatment using examiner's information and records of hospitals and mental health centers. After searching of antemortem information was fulfilled, 29 subjects who had met criteria of schizophrenia according to the Diagnostic and Statistical Manual of Mental Disorders (DSM-IV)[51] were selected. A toxicological screening for antipsychotics, other drugs and ethanol was performed on blood, urine, liver and gastric contents samples. All subjects who were drug-free at death (as revealed by the absence of prescriptions in medical histories) also gave negative results in the toxicological screening. The toxicological assays were performed at the National Institute of Toxicology, Madrid, Spain, using a variety of standard procedures including radioimmunoassay, enzymatic immunoassay, high-performance liquid chromatography and gas chromatography-mass spectrometry. Controls for the present study were chosen among the collected brains on the basis, whenever possible, of the following cumulative criteria: (i) negative medical information on the presence of neuropsychiatric disorders or drug abuse; (ii) appropriate sex, age, postmortem delay (time between death and autopsy), and freezing storage time to match each subject in the schizophrenia group; (iii) sudden and unexpected death (motor vehicle accidents); and (iv) toxicological screening for psychotropic drugs with negative results except for ethanol. Specimens of prefrontal cortex (Brodmann area 9) were dissected at autopsy (0.5-1 g tissue) on an ice-cooled surface and immediately stored at -80°C until use. The definitive pairs of antipsychotic-free schizophrenics and respective matched controls are shown in Supplementary Table 1, and the definitive pairs of atypical antipsychotic-treated schizophrenics and respective matched controls are shown in Supplementary Table 2. Pairs of schizophrenia and matched controls were processed simultaneously and under the

same experimental conditions. Tissue pH values were within a relatively narrow range (control subjects: 6.7 ± 0.08; schizophrenic subjects: 6.6 ± 0.06). Brain samples were also assayed for RIN (RNA integrity number) values using the Agilent 2100 Bioanalyzer (Applied Biosystems), as previously reported (control subjects: 7.87 ± 0.21; schizophrenic subjects: 7.61 ± 0.32).

Nuclei isolation and sorting via FACS

Nuclei isolation from frozen tissues (never fixed) of postmortem human brain samples was conducted using a published protocol[52] with some modifications Briefly, all steps were conducted on ice, and all centrifugation was conducted at 4 °C. One piece of brain tissue (~300 mg) was placed in 3 ml of ice-cold nuclei extraction buffer (NEB) [0.32 M sucrose, 5 mM $CaCl_2$, 3 mM $Mg(Ac)_2$, 0.1 mM EDTA, 10 mM Tris-HCl, and 0.1%(v/v) Triton X-100] with freshly added 30 μl of protease inhibitor cocktail (PIC, Sigma-Aldrich), 3 μl of 100 mM phenylmethylsulfonyl fluoride (PMSF, Sigma-Aldrich) in isopropyl alcohol, 3 μl of 1 M dithiothreitol (DTT, Sigma-Aldrich), and 4.5 μl of recombinant ribonuclease (RNase) inhibitor (2313A,Takara Bio). The tissue was homogenized in tissue grinder (D9063, Sigma-Aldrich). The homogenate was filtered with a 40 μm cell strainer (22-363-547, Thermo Fisher Scientific) and collected in a 15-ml centrifuge tube. The cell suspension was centrifuged at 1000 RCF at 4 °C for 10 min. The supernatant was discarded, and the pellet was resuspended in 0.5 ml of ice-cold NEB with freshly added 5 μl of PIC, 0.5 μl of PMSF, 0.5 μl of DTT, and 0.75 μl of RNase inhibitor. 500 μl of the sample was mixed with 750 μl of 50%(w/v) iodixanol (a mixture of 4 ml of OptiPrepTM gradient (Sigma-Aldrich) and 0.8 ml of diluent [150 mM KCl, 30 mM $MgCl_2$, and 120 mM Tris-HCl]). The mixture was centrifuged at 10,000 RCF at 4 °C for 20 min. Then, the supernatant was removed and 300 μl of 2%(w/v) normal goat serum (50062Z, Life technologies) in Dulbecco's PBS (DPBS, Life technologies) was added to resuspended the nuclei pellet. To label and separate $NeuN^+$ and $NeuN^-$ fractions, 6 μl of 2 ng/ml anti-NeuN antibody conjugated with Alexa 488 (MAB377X, Millipore) in DPBS was added into the nuclei suspension. The suspension was mixed well and incubated at 4 °C for 1 hour on a rotator mixer (Labnet). After incubation, the sample was sorted into $NeuN^+$ and $NeuN^-$ populations using a BD FACSARIATM Flow Cytometer (BD Biosciences). 400 μl of sorted nuclei suspension ($NeuN^+$ or $NeuN^-$), containing ~50000 nuclei (for conducting ChIP-seq and input libraries), was added into 600 μl of ice-cold PBS. 200 μl of 1.8 M sucrose solution, 5 μl of 1 M $CaCl_2$, and 3 μl of 1 M $Mg(Ac)_2$ were added into the mixture. The solution was mixed well and incubated on ice for 15 min. Then, the sample was centrifuged at 1800 RCF at 4 °C for 15 min. The supernatant was discarded and

the pellet was resuspended in 110 μl of PBS with freshly added 1.1 μl of PIC and 1.1 μl of PMSF and stored on ice until use.

Construction of ChIP-seq libraries

Chromatin fragments were prepared by using micrococcal nuclease (MNase) to digest sorted and concentrated nuclei ($NeuN^+$/$NeuN^-$) following a published protocol[25]. 54 μl of chromatin fragments (from 10,000 nuclei) was used in each ChIP assay. Chromatin immunoprecipitation was carried out using multiplexed MOWChIP assay[25] with anti-H3K4me3 (39159, Active Motif) and anti-H3K27ac (39135, Active Motif) antibody. ChIP-seq libraries were prepared using Accel-NGS 2S Plus DNA Library kit (Swift Biosciences) from the purified immunoprecipitated DNA. Minor modification was made to the manufacturer's procedures as detailed below. In the amplification step, instead of adding 10 μl of low EDTA TE buffer into each reactoin, we added the mixture of 7.5 μl of low EDTA TE buffer and 2.5 μl of 20X Evagreen dye to monitor and quantify PCR amplification. The reaction was stopped when the sample's fluorescence intensity increases by 3000 relative fluorescence units (RFU). Then, 50 μl of the mixture after PCR amplification was transferred into an Eppendorf tube and mixed with 37.5 μl of SPRIselect beads. After 5-min incubation at room temperature, the beads were conducted cleanup procedure with 80% ethanol. In the end, the DNA library was eluted from the beads into 7 μl of low EDTA TE buffer.

Construction of RNA-seq libraries

100 μl of sorted nuclei suspension ($NeuN^+$ or $NeuN^-$) from brain tissue, containing ~12,000 nuclei for producing 2 replicate libraries, was used for RNA extraction by using the RNeasy Mini Kit (74104, Qiagen) and RNase-Free DNase Set (79254, Qiagen), following the manufacturer's instruction. Half of the extracted mRNA (from 6,000 nuclei) in 30-μl volume was concentrated by ethanol precipitation and resuspended in 4.6 μl of RNase-free water. mRNA-seq libraries were prepared using Smart-seq2[26] and a Nextera XT DNA Library Preparation kit (FC-131-1024, Illumina) following the protocol and the manufacturer's instructions with minor modification. ~2 ng of mRNA (in 4.6 μl of water) was mixed with 2 μl of 100 mM oligo-dT primer and 2 μl of 10 mM dNTP mix. After being denatured at 72 °C for 3 min, the mRNA solution was immediately placed on ice. Then, 11.4 μl of reverse transcript mix [1 μl of SuperScript II reverse transcriptase (200 U/ml), 0.5 μl of RNAse inhibitor (40 U/ml), 4 μl of Superscript II first-strand buffer, 1 μl of DTT (100mM), 4 μl of 5 M Betaine, 0.12 μl of 1 M $MgCl_2$, 0.2 μl of TSO (100 mM),

0.58 μl of nuclease-free water] was mixed with the mRNA solution and the mixture was incubated at 42 °C for 90 min, followed by 10 cycles of (50 °C for 2 min, 42 °C for 2 min). The reaction was finally inactivated at 70 °C for 15 min. 20 μl of first-strand mixture was then mixed with 25 μl of KAPA HiFi HotStart ReadyMix, 0.5 μl of (100 mM) IS PCR primers, 0.5 μl of Evagreen dye, and 4 μl of nuclease-free water. Generated complementary DNA (cDNA) was amplified by incubated at 98 °C for 1 min, followed by 9-11 cycles of (98 °C 15 s, 67 °C 30 s, 72 °C 6 min). After PCR amplification, 50 μl of PCR mix was purified by using 50 μl of SPRIselect beads. ~600 pg of purified cDNA was used for Nextera XT library preparation. ChIP-seq and RNA-seq library fragment size were measured by using high sensitivity DNA analysis kit (5067-4626, Agilent) on a TapeStation system (2200, Agilent). The concentration of each library was examined by a KAPA library quantification kit (KK4809, Kapa Biosystems), and then the quantified libraries were pooled at 10 nM. The libraries were sequenced by Illumina HiSeq 4000 with single-end 50-nt readAround 15 million reads were generated for each ChIP-seq library, 10 million reads for each input library, 11 million reads were generated for RNA-seq library.

ChIP-seq data processing

Raw ChIP-seq reads and input data, were mapped to human genome (GRCh38) using BWA (0.7.7-r441). Peaks were called using MACS2 (2.1.0.20150420.1) using a p-value cutoff of 0.01 for the narrow marks (H3K4me3 and H3K27ac).

RNA-seq data processing

The human genome (GRCh38) and comprehensive gene annotation were obtained from GENCODE (v29). RNA-seq reads were mapped with STAR (2.7.0f) and quantified with RSEM (v1.3.1) using the default parameters.

Differential analysis for ChIP-seq data

The peaks were called using MACS2[53]. The peaks with p-value<0.05 were taken as input for diffBind R package. Using the function of dba.peakset in diffbind, “majority-rules” was applied to generate consensus peak set for both SCZ and CTL groups (i.e. a consensus peak must be present in more than half of the replicate datasets) and then the two consensus peak sets were combined into a master set for analysis. The raw read counts were extracted using the function of dba.count in diffBind, and DESeq2 R package was used to perform the differential peaks analysis based on the raw read counts to identify differential peaks between the two consensus peak sets (FDR<0.05).

Differential analysis for RNA-seq data

The raw read counts for all genes were taken as input for DESeq2 for differential analysis. The genes with FDR <0.05 were called differential expressed genes.

Taiji pipeline

Active regulatory elements were first identified via the overlap of high confidence peaks from H3K27ac with known gene promoter regions (4kbp upstream and 1kbp downstream of the transcription start sites). The distal H3K27ac peaks were assigned to active promoters using the unsupervised learning method EpiTensor, and assigned as an enhancer-promoter interaction if one locus overlapped with the distal peak and the other locus in the pair overlapped with a known promoter. Putative TF binding motifs were curated from the CIS-BP database[54]. Using FIMO's algorithm[55]. TFs were identified as having binding sites within 150-bp regions centered around ATAC-seq peak summits. 58 unique $NeuN^+$ (29 schizophrenia and 29 control) and 58 unique $NeuN^-$ (29 schizophrenia and 29 control) network topologies were thus constructed by forming directed edges between TF and their regulatees, if the TF had a predicted binding site in the gene's promoter or linked enhancer.

Personalized PageRank (PPR)

The Personalized PageRank (PPR) algorithm was run to measure the global influence of each node. To initialize the networks, node weights were assigned according to the relative gene expression normalized across all samples. Edge weights were determined according to the expression level of the parent node TF and the pooled H3K27ac ChIP-seq peak intensity (strength of the TF-gene association) as previously reported[32]. The directionality of the topological edges was reversed and the normalized node weights were then used as the seed vector for the PPR calculation. Post convergence, edge directionality was re-reversed.

EpiSig analysis

To integrate H3K27ac, H3K4me3 and RNA-seq data from two cell types across the postmortem frontal cortex samples from schizophrenia subjects and controls, EpiSig was employed[31]. This algorithm detects the significant signals from sequencing data in 5kb bins across the whole genome, and then clusters the regions based on the similar epigenomic profiles across all samples.

Age correlation analysis

Raw expression, pairwise expression and pairwise TF PPR age correlations were calculated using the Pearson R correlation. Significance was assessed by calculating p-values for the Pearson R correlations using the t-distribution with n-2 degrees of freedom for the respective cohort.

Extended Data Figure legends and Supplementary Tables

Extended Data Fig. 1 | Differential histone modification peaks and DEGs obtained by comparing the AF-schizophrenia (**a**) or AT-schizophrenia (**b**) groups and their respective controls. The differential peaks or DEGs were identified using FDR < 0.05.

Extended Data Fig. 2 | Differential peak enrichment analysis for antipsychotic-free neurons in EpiSig clusters. a, Percentage of total AF-specific differential H3K27ac peaks in the 22 significantly enriched (FDR<0.05) *EpiSig* clusters. Top 3 clusters 630, 732 (Section 1) and 449 (Section 2) highlighted in red. Differential peaks (all cluster regions for clusters with less than 10 differential peaks) mapped to 166 genes using GREAT with default settings. Histograms of ln[distance to tss] and peak width for 36 H3K27ac differential peaks and 72 regions in cluster 449 (median distance to tss 210 kbp). **b,** Percentage of total AF-specific differential H3K4me3 peaks in the 22 significantly enriched (FDR<0.05) *EpiSig* clusters. Top 3 clusters 582 (Section 6), 270 and 259 (Section 2) highlighted in red. Differential peaks (all cluster regions for clusters with less than 10 differential peaks) mapped to 128 genes using GREAT with default settings. Histograms of ln[distance to tss] and peak width for 19 H3K27ac differential peaks (median distance to tss 186 kbp) and 16 H3K4me3 differential peaks (median distance to tss 141 kbp). **c,** Functional enrichment analysis for the union of gene sets (294 genes) (supplementary Table 9).

Extended Data Fig. 3 | Differential peak enrichment analysis for antipsychotic-treated neurons in EpiSig clusters. a, Percentage of total at-specific differential H3K27ac peaks in the 99 significantly enriched (FDR<0.05) *EpiSig* clusters. Top 2 clusters 6 and 8 (Section 4) highlighted in red. Differential peaks mapped to 794 genes using GREAT with default settings. Histograms of ln[distance to tss] and peak width for 623 H3K27ac differential peaks showing bimodal proximal/distal distribution. **b,** Percentage of total AT-specific differential H3K4me3 peaks in the 99 significantly enriched (FDR<0.05) *EpiSig* clusters. Top 2 clusters 79 (Section 3) and 112 (Section 6) highlighted in red. Differential peaks mapped to 80 genes using GREAT with default settings. Histograms of ln[distance to tss] and peak width for 19 H3K27ac differential peaks (median distance to tss 83 kbp) and 37 H3K4me3 differential peaks (median

distance to tss 142 kbp). **c,** Functional enrichment analysis for the H3K4me3 differential peak gene set (80 genes) (supplementary Table 10).

Supplementary Table 1 | Demographic information of AF-schizophrenia subjects and controls

Supplementary Table 2 | Demographic information of AT-schizophrenia subjects and controls

Supplementary Table 3 | RNA-seq analysis of $NeuN^+$ and $NeuN^-$ nuclei samples from the frontal cortex of 29 control subjects.

Supplementary Table 4 | Histone marks H3K27ac and H3K4me3 and transcriptomes in neuronal and glial nuclei from the frontal cortex of schizophrenia subjects and controls

Supplementary Table 5 | *EpiSig* analysis in neuronal and glial nuclei from the frontal cortex of schizophrenia subjects and controls

Supplementary Table 6 | *Taiji* analysis in neuronal and glial nuclei from the frontal cortex of schizophrenia subjects and controls

Supplementary Table 7 | Histone marks H3K27ac and H3K4me3 and transcriptomes in neuronal and glial nuclei from the frontal cortex of AF-schizophrenia subjects, AT-schizophrenia subjects and controls

Supplementary Table 8 | *Taiji* analysis in neuronal and glial nuclei from the frontal cortex of AF-schizophrenia subjects, AT-schizophrenia subjects and controls

Supplementary Table 9 | *EpiSig* analysis in neuronal and glial nuclei from the frontal cortex of AF-schizophrenia subjects and controls

Supplementary Table 10 | *EpiSig* analysis in neuronal and glial nuclei from the frontal cortex of AT-schizophrenia subjects and controls

Supplementary Table 11 | Effect of age on chromatin organization in the frontal cortex of AF-schizophrenia subjects, AT-schizophrenia subjects and controls

Supplementary References

51 American Psychiatric Association, *Diagnostic and Statistical Manual of Mental Disorders: DSM-IV 4th edition*. (Washington, DC, 1994).

52 Lake, B. B. *et al.* Neuronal subtypes and diversity revealed by single-nucleus RNA sequencing of the human brain. *Science* **352,** 1586-1590 (2016).

53 Zhang, Y. *et al.* Model-based analysis of ChIP-Seq (MACS). *Genome Biol* **9,** R137 (2008).

54 Weirauch, M. T. *et al.* Determination and inference of eukaryotic transcription factor sequence specificity. *Cell* **158,** 1431-1443 (2014).

55 Grant, C. E. *et al.* FIMO: scanning for occurrences of a given motif. *Bioinformatics* **27,** 1017-1018 (2011).

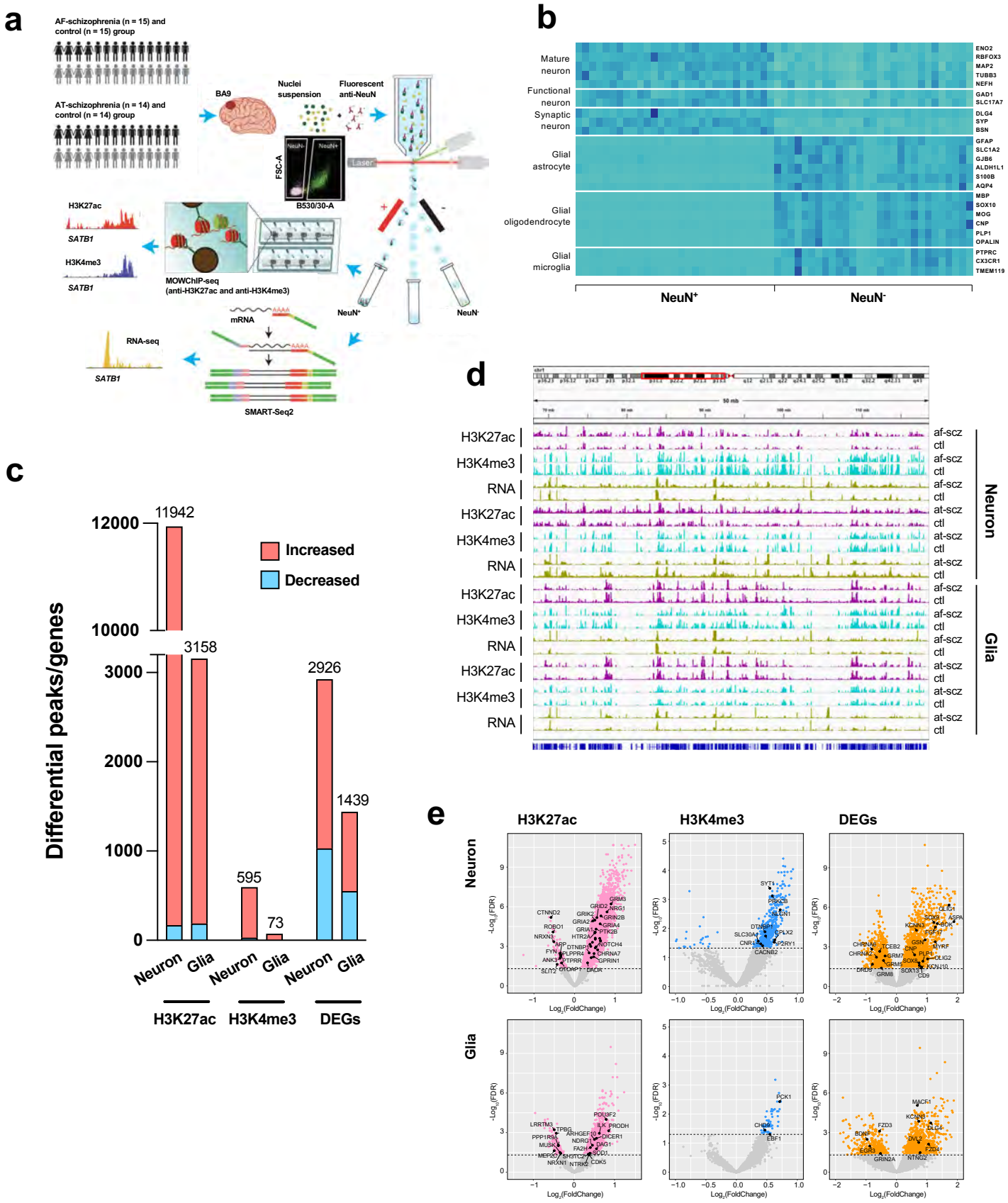

Zhu, Ainsworth et al (Fig. 1)

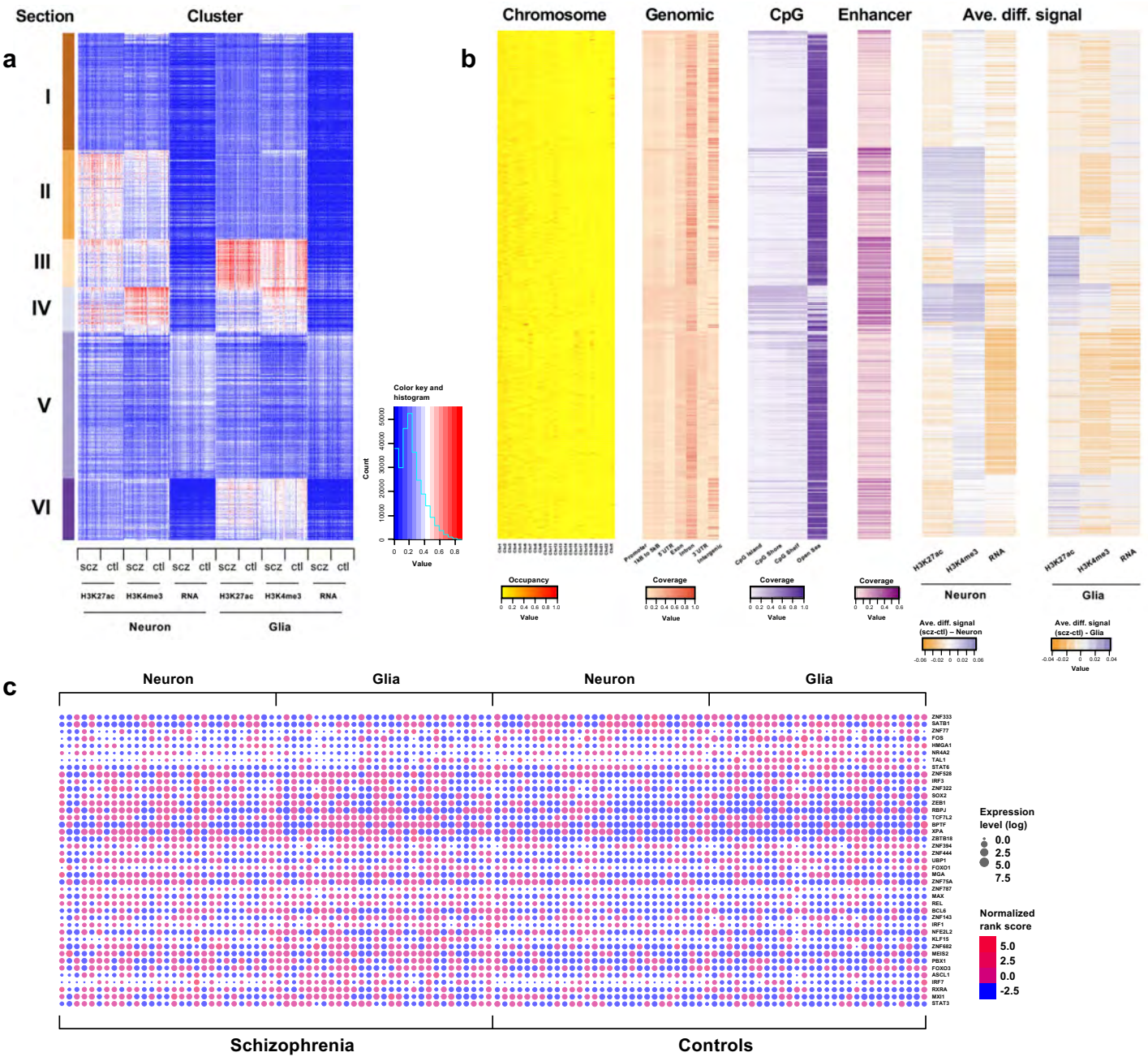

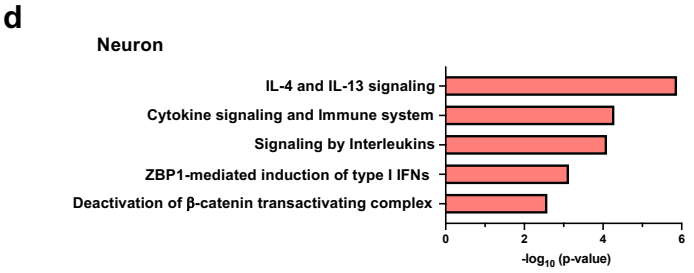

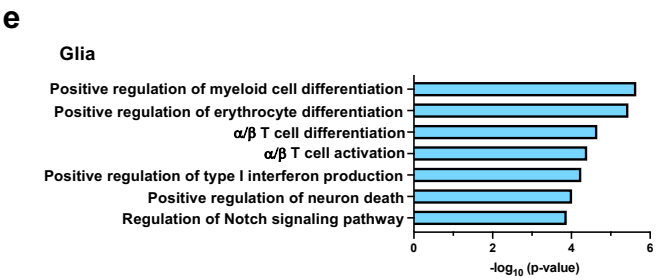

Zhu, Ainsworth et al (Fig. 2)

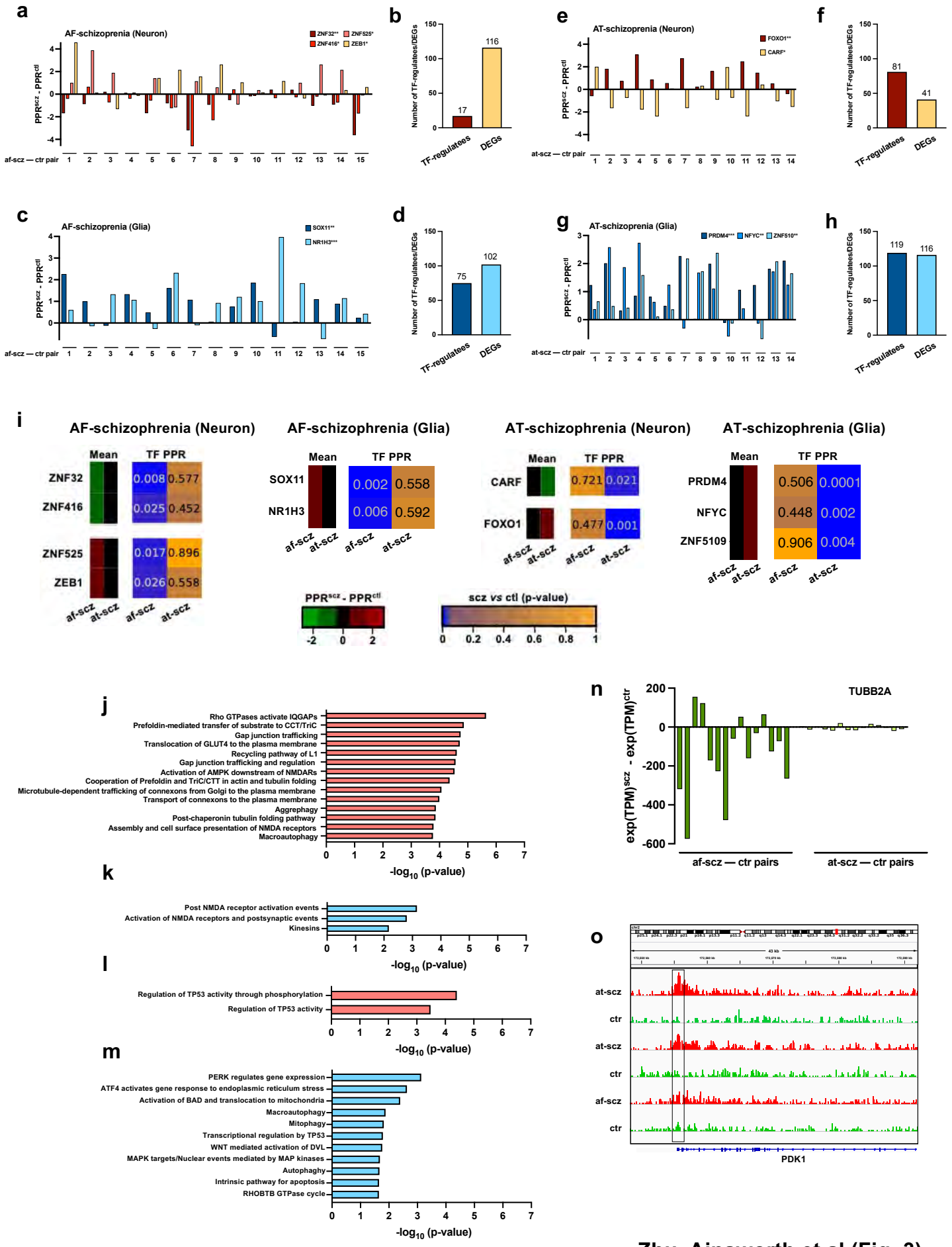

Zhu, Ainsworth et al (Fig. 3)

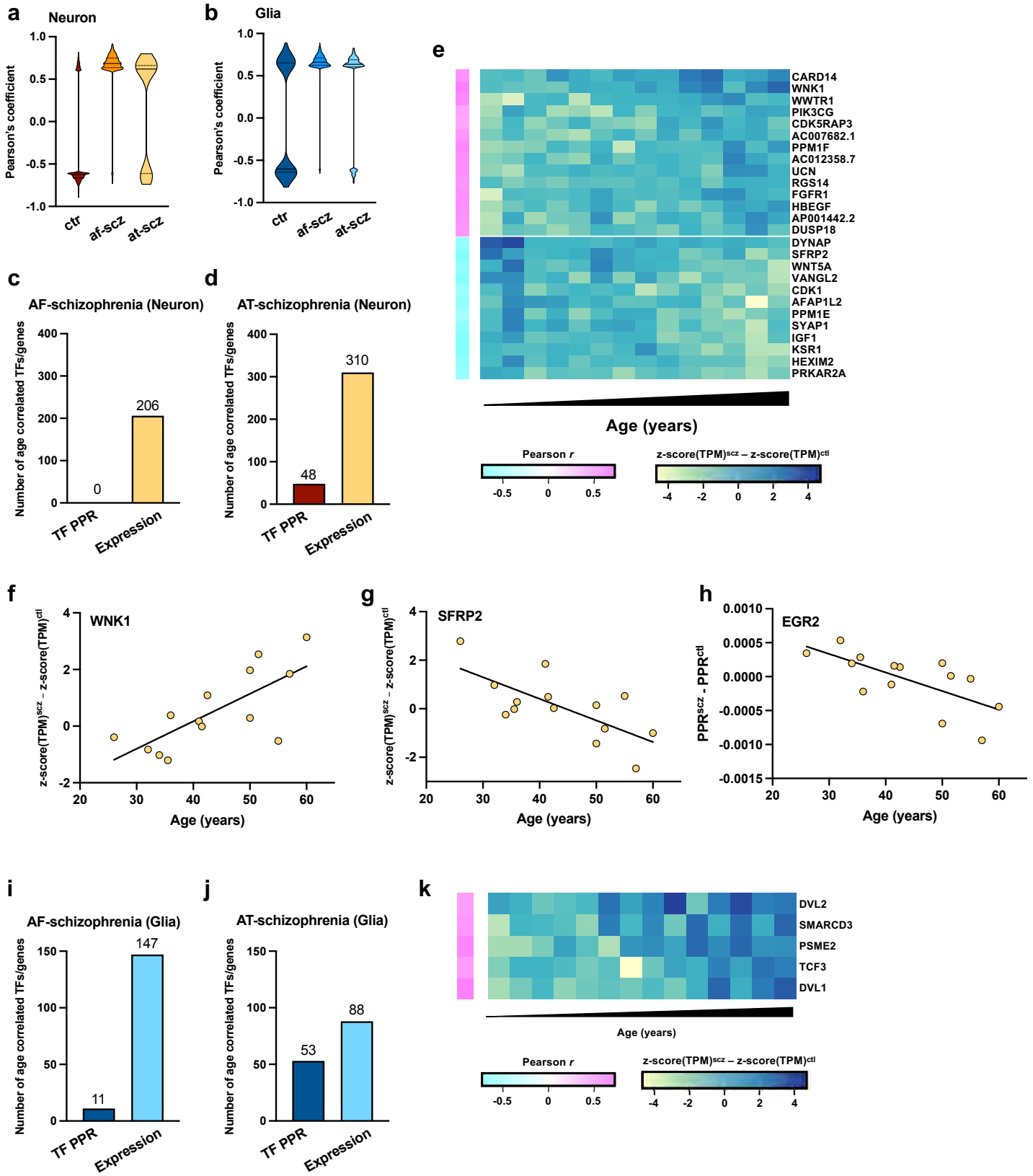

Zhu, Ainsworth et al (Fig. 4)